Available online at www.sciencedirect.com
SCIENCE DIRECT
International Journal of Heat and Mass Transfer 49 (2006) 2347–2355
International Journal of HEAT and MASS TRANSFER
www.elsevier.com/locate/ijhmt

Detailed numerical simulation of thermal radiation influence in Sandia flame D

Xiao Xu *, YiLiang Chen, Haifeng Wang

Department of Thermal Science and Energy Engineering, University of Science and Technology of China, Hefei, Anhui 230027, People's Republic of China

Received 30 May 2005; received in revised form 17 November 2005
Available online 3 February 2006

Abstract

In order to investigate the influence of thermal radiation in turbulent combustion processes, Sandia flame D is numerically simulated, with multiple-time scale (MTS) k–ε turbulence model for turbulence, the combination of probability density function (PDF) transportation method, Lagrangian flamelet model (LFM) and the detailed chemical reaction mechanism GRI 3.0 (consisting of 53 species and 325 elemental reactions) for combustion and finite volume/correlated-k (FV/CK) method for radiation heat transfer. To account for turbulence's influence on radiation, the effects of turbulence–radiation interactions (TRI) are investigated in radiation calculations and it is recommended that for detailed numerical simulation TRI should be considered. Numerical results with and without radiation influence being taken into accounted are compared with experimental data. Different from reports by other researchers, our simulation results show that although the magnitude of thermal radiation is relatively small, its influence on combustion process is significant. It is suggested that turbulence and chemical reactions may magnify the influence of thermal radiation.

Keywords: Sandia flame D; PDF; LFM; FVM; Correlated-k; TRI

1. Introduction

A lot of efforts have been devoted to numerical simulation of flames and commercial combustion systems, in many cases of which thermal radiation may be an important heat transfer mode. However, to simulate thermal radiation in combustion processes accurately, there are several fundamental difficulties to overcome. First, the treatment of turbulent reacting flows itself is a challenging task [1,2]. Secondly, a solver of radiative transfer equation (RTE) which can be easily incorporated into CFD code is required. Thirdly, the radiative properties of real (non-gray) gases need to be determined. Finally, accurate prediction of influences of turbulence–radiation interaction (TRI) is necessary.

Although PDF transportation methods [3] significant advantage of exact treatment of chemical reactions is well known, the pure PDF method is rather computation expensive, especially when a detailed chemical mechanism such as GRI 3.0 [4] is implemented. In the present paper, a much more economical combustion submodel, namely the Lagrangian flamelet model [5] is used together with PDF transportation equation of mixture fraction to simulate the combustion process.

Up to date, there are many explored RTE solvers [6]. Among all these solvers, both DOM and FVM can be easily incorporated into CFD codes and FVM is the choice of the present work. Along with FVM, the correlated-k distribution (CK) method, which assumes absorption coefficient as the basic radiative property, is used to calculate the absorption coefficients of the radiative medium. The parameters for CK model are provided by EM2C [7].

The effect of turbulence–radiation interactions (TRI) has long been known. To the authors' best knowledge,

* Corresponding author. Tel.: +86 551 3601650; fax: +86 551 3606459.
E-mail address: xuxiao@mail.ustc.edu.cn (X. Xu).

0017-9310/$ - see front matter © 2006 Elsevier Ltd. All rights reserved.
doi:10.1016/j.ijheatmasstransfer.2005.11.017

Nomenclature

$c_{p\alpha}$	specific heat capacity of species α
c_p	specific heat capacity of the mixture
d	diameter of fuel jet nozzle for Sandia flame D
$\tilde{f}$	PDF of mixture fraction
g	cumulative distribution function of absorption coefficient
I_η	spectral radiative intensity
$I_{b\eta}$	spectral Plank function
J_i	molecular diffusive flux of mixture fraction
k	turbulent kinetic energy, $=k_p + k_t$
k_p	turbulent kinetic energy of large eddies in production range
k_t	turbulent kinetic energy of fine-scale eddies in dissipation range
k	absorption coefficient
k_η	spectral absorption coefficient
k_i^*	parameters of the correlated k-distribution model
L, M	total number of discrete polar and azimuthal angle
N_b	total number of molecular gas bands
N_Q	total number of quadrature points in each gas band
Q	partial function of an isolated absorbing molecule
S_α	reaction rate
S_R	rate of radiative heat loss per unit volume
T	temperature
t	time
W_H, W_C	atomic weight of the element H and O
x, r	cylindrical coordinates
X_s	molar partial pressure of s species
Y_α	mass fraction of species α
Y_H, Y_C	mass fraction of element H and O

Greek symbols

$\alpha_{m+1/2}$, $\alpha_{m-1/2}$	coefficients for angular-distribution term
ε_p	energy transfer rate from production range to dissipation range
ε, ε_t	dissipation rate of turbulent kinetic energy
μ_t	turbulent eddy-viscosity
ξ	mixture fraction
χ	scalar dissipation rate
ρ	density
$\bar{\rho}$	mixture density
Ω	solid angle
ξ^{lm}	direction-cosines of the axial direction
μ^{lm}	radial tangential direction
η^{lm}	tangential direction
$\Delta\eta$	wavenumber interval
ω_i	ith quadrature weight in the correlated k-distribution method
θ	polar angle measured from $\hat{e}_z$
ϕ	azimuthal (planar) angle measured from $\hat{e}_x$

Superscripts

1, 2	inlet of fuel and oxidant
l, m	angular direction

Subscripts

b	black-body
η	wavenumber
i	values at ith quadrature points
k	kth narrow band
st	stoichiometric condition

Mazumder and Modest are the first ones to present the idea of treating turbulence–radiation interactions by PDF/MC method [8]. Li and Modest [9], with the aid of FLUENT, investigated TRI in gaseous flames. In both works, a simplified reaction mechanism is chosen for the chemical reaction rate and P_1 is used to solve the RTE. In the present work, TRI is fully taken into accounted when doing radiation calculations and its influence on thermal radiation is briefly discussed as well.

Sandia flame D is selected here as the simulation case for the reason that organizers of the international workshop on computation of turbulent non-premixed flames (TNF) have recommended to consider radiation effects in the simulation of Flame D, especially when NO levels are to be predicted [10]. And there are some related research reports [11–13], which can be used as comparisons for our own research. The main purpose of this paper is to investigate the influence of thermal radiation on combustion calculations.

2. Mathematical modeling

For Sandia flame D, turbulent transportations along the axis are much larger than those of the radial direction, which justifies the flow being formulated into the boundary layer form. The flow can be described by parabolized Navier–Stokes (PNS) equation, which, in cylindrical coordinate system, can be written as

$$\frac{\partial(r\bar{\rho}\tilde{u})}{\partial x} + \frac{\partial(r\bar{\rho}\tilde{v})}{\partial r} = 0 \tag{1}$$

$$\bar{\rho}\tilde{u}\frac{\partial\tilde{u}}{\partial x} + \bar{\rho}\tilde{v}\frac{\partial\tilde{u}}{\partial r} = \frac{1}{r}\frac{\partial}{\partial r}\left(r\mu_t\frac{\partial\tilde{u}}{\partial r} + (\rho_\infty - \bar{\rho})g\right) \tag{2}$$

2.1. Turbulence model

A multiple-time scale (MTS) k–ε turbulence model [14] is used for the turbulence calculation. The concept of the

MTS k–ε model is that the turbulent kinetic energy spectrum can be partitioned into two regions, i.e. the production region and the dissipation region. The total turbulent kinetic energy consists of the large-eddy energy in the production range and the fine-scale-eddy energy in the dissipation range ($k = k_p + k_t$). The large-eddy energy k_p is generated by the mean flow instability and cascades to finer eddies with a transfer rate of ε_p while the finer-scale-eddy energy k_t is dissipated into thermal energy by viscous forces with a dissipation rate of ε_t. The turbulence eddy viscosity is defined as

$$\mu_t = \bar{\rho} C_{\mu f} k^2/\varepsilon_p \tag{3}$$

where $C_{\mu f} = 0.09$.

The performance of MTS k–ε turbulence model for axisymmetric turbulence jet flame has been examined in [15], where the transport equations for k_p, k_t, ε_p and ε_t can be found as well.

2.2. Combustion model

The Lagrangian flamelet model together with PDF transportation equation for mixture fraction is applied for the simulation of combustion process.

The flamelet model is based on the idea that a turbulent flame may be regarded as an ensemble of flamelet structures attached to the instantaneous position of the flame surface, which is corrugated by the turbulent flow field. According to Peters [16], the flamelet structure may be calculated by solving the flamelet equations. When assuming the Lewis number for all the species being 1, the flamelet equations may be written as

$$\rho\frac{\partial Y_\alpha}{\partial t} - \rho\frac{\chi}{2}\frac{\partial^2 Y_\alpha}{\partial \xi^2} - S_\alpha = 0 \tag{4}$$

$$\rho\frac{\partial T}{\partial t} - \rho\frac{\chi}{2}\frac{\partial^2 T}{\partial \xi^2} + \sum_{\alpha=1}^{h_\alpha} S_\alpha - \sum_{\alpha=1}^{\sigma-1}\rho\frac{\chi}{2}\frac{c_{p\alpha}}{c_p}\frac{\partial Y_\alpha}{\partial \xi} - \rho\frac{\chi}{2c_p}\frac{\partial T}{\partial \xi}\frac{\partial c_p}{\partial \xi} - \frac{S_R}{c_p} = 0 \tag{5}$$

where T is the temperature, Y_α the mass fraction of species α, ρ the density, χ the scalar dissipation rate, $c_{p\alpha}$ the specific heat capacity of species α, c_p the specific heat capacity of the mixture, t the time, S_α the reaction rate, S_R the rate of radiative heat loss per unit volume and ξ the mixture fraction, which is defined as [16]:

$$\xi = \frac{(Y_H - Y_{H,2})/2W_H + (Y_C - Y_{C,2})/2W_C}{(Y_{H,1} - Y_{H,2})/2W_H + (Y_{C,1} - Y_{C,2})/2W_C} \tag{6}$$

where Y_H and Y_C denote mass fractions of element H and O, W_H and W_C denote atomic weights of the element H and O and the subscripts 1 and 2 indicate the inlet of fuel and oxidant, respectively.

The scalar dissipation rate χ in Eqs. (4) and (5) is a function of the mixture fraction and may be taken from counter-flow geometry as [16]:

$$\chi = \chi_{st}\cdot Q(\xi) = \chi_{st}\cdot \exp\{-2[\mathrm{erfc}^{-1}(2\xi)]^2\}/\exp\{-2[\mathrm{erfc}^{-1}(2\xi_{st})]^2\} \tag{7}$$

where erfc^{-1} is the inverse of the complementary error function and the subscript st corresponds to stoichiometric condition.

It can be seen from the above that after the initial boundary conditions are given, the flamelet structure is determined:

$$\tilde{\phi} = \tilde{\phi}(t, \xi, \chi_{st}) \tag{8}$$

According to Pitsch [5], the time t that appears in the flamelet equations can be written as

$$t = \int_0^x \{\tilde{u}(x) \mid \tilde{\xi} = \xi_{st}\}^{-1}\,\mathrm{d}x \tag{9}$$

The conditional mean scalar dissipation rate for the stoichiometric mixture in each computation cell can be expressed as

$$\widehat{\chi_{st}} = \frac{\int_V \tilde{\chi}_{st}^{3/2}\bar{\rho} f(\xi_{st})\,\mathrm{d}V}{\int_V \tilde{\chi}_{st}^{3/2}\bar{\rho} f(\xi_{st})\,\mathrm{d}V} \tag{10}$$

with $\tilde{\chi}_{st}$ being calculated according to

$$\tilde{\chi}_{st} = C_\phi \frac{\varepsilon}{k}\widehat{\xi''^2}\Big/\int_0^1 \Big(\exp\{-2[\mathrm{erfc}^{-1}(2\xi)]^2\} \Big/ \exp\{-2[\mathrm{erfc}^{-1}(2\xi_{st})]^2\}\Big)\tilde{f}(\xi)\,\mathrm{d}\xi \tag{11}$$

By now, the mean structure of flamelet can be written in the form as

$$\tilde{\phi} = \int_0^1 \phi(\xi, \widehat{\chi_{st}}, t)\tilde{f}(\xi)\,\mathrm{d}\xi \tag{12}$$

where $\tilde{f}(\xi)$ is the PDF of mixture fraction. Other than assuming the mixture fraction being of a certain distribution as [11], here, the PDF transportation equation for mixture fraction is solved:

$$\frac{\partial(\bar{\rho}\tilde{f})}{\partial t} + \frac{\partial}{\partial x_i}(\bar{\rho}\tilde{u}_i\tilde{f}) + \frac{\partial}{\partial x_i}(\bar{\rho} < u_i'' \mid \psi > \tilde{f}) + \frac{\partial}{\partial \xi}\left[\left\langle -\frac{\partial J_i}{\rho\partial x_i}\middle|\xi\right\rangle\bar{\rho}\tilde{f}\right] = 0 \tag{13}$$

The third term on the right hand side of Eq. (13) stands for turbulent mixing and the fourth term stands for small-scale mixing, which is the only term requires modeling in the PDF equation. In the present work, the small-scale mixing is modeled by the EMST model [17].

As has been mentioned, the flow we are now dealing with is a parabolized flow, which means all scalar information cannot be known before the whole computation domain is scanned. However, except for using optically thin approximation, radiation calculation must be based on information of the whole computation domain. In order to compromise this contradiction, iterations are introduced. That is, in the first round calculation, Eqs. (1)–(5) and 13 are calculated with optically thin approximation

being used for the treatment of radiation source term in Eq. (5). After computations for the whole computation domain are done, FVM/CK is applied to derive the "real" radiation source term with absorb radiation being included, which will be stick back into flamelet equation and later, another round of calculation (iteration) will be done. For the present problem, two iterations will be sufficient.

2.3. The correlated-k distribution (CK) model

The physical basis of CK model is the fact that over a small spectral interval Plank function remains essentially constant while the absorption coefficient varies widely, attaining the same value many times at slight different wavenumbers. So that what is important is the probability density function that the absorption coefficient takes a distinct value across the band. The probability density function $f(k)$ can be calculated as

$$f(k) = \frac{1}{\Delta\eta}\int_{\Delta\eta}\delta(k-k_\eta)\,\mathrm{d}\eta \tag{14}$$

For details of the CK model, Refs. [6,7] are recommended.

By applying CK model, over each narrow band $\Delta\eta$, the absorption coefficient $k(\eta)$ can be replaced by an N-point Gaussian quadrature, defined by quadrature points g_i and whose associated weights ω_i:

$$\bar{k}(\eta) = \int_0^1 k(g)\,\mathrm{d}g \approx \sum_{i=1}^{N_\mathrm{Q}}\omega_i k(g_i) \tag{15}$$

where N_Q is the number of quadrature points in each narrow band.

Model parameters are then values which, at atmospheric pressure, depend on the temperature, the narrow band intervals, and particularly, the molar fraction of associated radiation medium:

$$k(g_i) = X_s p_s k_i^*/(TQ(T)) \tag{16}$$

where p_s equals 1 atm, X_s stands for the molar fraction of corresponding radiation medium and $Q(T)$ represents partition function of corresponding radiation medium.

For the present case, CO_2 and H_2O are taken as the radiating gases and the contribution from other radiating species, such as CO and CH_4, is neglected since CK parameters for CO and CH_4 are not available to us. According to[11], the role of CO is negligible in the backward part of the flow while it may contribute to an increase of the radiation intensity by about 2.5% in the forward part of the flow. The contribution of CH_4 is less than that of CO. For gas mixture of H_2O and CO_2, there are a number of overlapping narrow bands at which both gases absorb and emit radiation. According to [18], it is justified to assume that the spectrums of H_2O and CO_2 are independent of each other for narrow band intervals. Therefore, the total absorption coefficient at each common quadrature point equals the absorption coefficient of H_2O plus that of CO_2.

2.4. FVM/CK and treatment for overlapping bands

A detailed description of FVM can be found in other publication [6].

In cylindrical coordinates system, for the specific solid angle $\mathrm{d}\Omega^{lm}$, the discrete RTE can be written as

$$\mu^{lm}\frac{\partial I^{lm}_{i,\Delta\eta_k}}{\partial x} + \frac{\xi^{lm}}{r}\frac{\partial(rI^{lm}_{i,\Delta\eta_k})}{\partial r} - \frac{1}{r}\frac{\partial}{\partial\psi}(\eta^{lm}I^{lm}_{i,\Delta\eta_k}) = -k_i I^{lm}_{i,\Delta\eta_k} + k_i I_{\mathrm{b},\Delta\eta_k} \tag{17}$$

where $I^{lm}_{i,\Delta\eta_k}$ is the averaged radiation intensity over the kth band for quadrature points i in the direction specified by solid angle Ω^{lm}. If kth band is an overlapping band of H_2O and CO_2, then:

$$k_i = k_{\mathrm{h},i} + k_{\mathrm{c},i} \tag{18}$$

where $k_{\mathrm{h},i}$ and $k_{\mathrm{c},i}$ are absorption coefficient of H_2O and CO_2 for quadrature point i, respectively.

And ξ^{lm}, μ^{lm} and η^{lm} are direction-cosines of the axial, radial and tangential direction, respectively:

$$\mu^{lm} = \sin\theta_l\cos\psi_m, \quad \xi^{lm} = \sin\theta_l\sin\psi_m, \quad \eta^{lm} = \cos\theta_l \tag{19}$$

where θ is the polar angle and ϕ the azimuthal angle measured from the local radial direction.

The boundary of computational domain is treated as blackbody at room temperature:

$$I_{w,i} = I_{\mathrm{b}w} \tag{20}$$

The total radiation intensity for solid angle $\mathrm{d}\Omega^{lm}$ is

$$I^{lm} = \sum_{n=1}^{N_\mathrm{b}}\Delta\eta_k\sum_{i=1}^{N_\mathrm{Q}}\omega_i I^{lm}_{i,\Delta\eta_k} \tag{21}$$

where N_b stands for the total number of bands.

In order to account for TRI, Eq. (17) is time averaged, yielding:

$$\mu^{lm}\frac{\partial\overline{I^{lm}_{i,\Delta\eta_k}}}{\partial x} + \frac{\xi^{lm}}{r}\frac{\partial(r\overline{I^{lm}_{i,\Delta\eta_k}})}{\partial r} - \frac{1}{r}\frac{\partial}{\partial\psi}(\eta^{lm}\overline{I^{lm}_{i,\Delta\eta_k}}) = -\overline{k_i I^{lm}_{ij,\Delta\eta_k}} + \overline{k_i I_{\mathrm{b},\Delta\eta_k}} \tag{22}$$

A most common yet rigorous treatment of TRI is the optically thin-eddy approximation proposed by Kabashnikov and Myasnikova [19], which is based on the assumption that individual eddies are homogeneous, optically thin and statistically independent. Under the approximation, the correlation between fluctuations of the absorption coefficient and fluctuations of the radiation intensity can be treated in a simplified way:

$$\overline{k_i I^{lm}_{i,\Delta\eta_k}} \sim \bar{k}_i\bar{I}^{lm}_{i,\Delta\eta_k} \tag{23}$$

The third term on the left hand of Eq. (20) is called angular-distribution term, which, for certain η^{lm}, can be discretized as following:

$$\frac{\partial}{\partial\psi}(\eta^{lm}\overline{I}^{lm}_{i,\Delta\eta_k}) \approx (\alpha_{m+1/2}\overline{I}^{l(m+1/2)}_{i,\Delta\eta_k} - \alpha_{m-1/2}\overline{I}^{l(m-1/2)}_{i,\Delta\eta_k})/\Delta\psi \quad (24)$$

here, the coefficient $\alpha_{m+1/2}$ and $\alpha_{m-1/2}$ are defined as

$$\alpha_{m+1/2} = \alpha_{m-1/2} = (\cos(2\theta_l - \Delta\theta) - \cos(2\theta_l + \Delta\theta))/4 \quad (25)$$

With the help of step discretization scheme:

$$\overline{I}^{lm}_{i,\Delta\eta_k,x,\text{out}} = \overline{I}^{lm}_{i,\Delta\eta_k,r,\text{out}} = \overline{I}^{l(m+1/2)}_{i,\Delta\eta_k,p} = \overline{I}^{lm}_{i,\Delta\eta_k,p} \quad (26)$$

Eq. (20) is integrated over a controlled volume and solid angle and finally yields:

$$\begin{aligned} &|\mu^{lm}| A_x(\overline{I}^{lm}_{i,\Delta\eta_k,x,\text{out}} - \overline{I}^{lm}_{i,\Delta\eta_k,x,\text{in}}) \\ &+ |\xi^{lm}| [A_{r,\text{out}}\overline{I}^{lm}_{i,\Delta\eta_k,r,\text{out}} - A_{r,\text{in}}\overline{I}^{lm}_{i,\Delta\eta_k,r,\text{in}}] \\ &- |A_{r,\text{out}} - A_{r,\text{in}}| \frac{\alpha_{m+1/2}\overline{I}^{l(m+1/2)}_{i,\Delta\eta_k,p} - \alpha_{m-1/2}\overline{I}^{l(m-1/2)}_{i,\Delta\eta_k,p}}{\Delta\psi} \\ &= (\overline{k_i I_{\text{b},\Delta\eta_k}} - \bar{k}_i\overline{I}^{lm}_{i,\Delta\eta_k,p})V_P\Delta\Omega^{lm} \end{aligned} \quad (27)$$

where A are the areas of the cell faces and V is the volume of cells. The indices in (out) denote a cell face where radiation flows into (out from) the control volume and the subscripts r and x stand for the radial and axial directions, respectively. The subscript P identifies the control volume under consideration. For numerical solution of Eq. (27), a scan algorithm is adopted [6].

Finally, the radiation source term can be calculated as

$$S_R = \overline{\nabla\cdot q} = \sum_{n=1}^{N_b}\Delta\eta_k\sum_{i=1}^{N_Q}\omega_i\left(4\pi\overline{k_i I_{\text{b},\Delta\eta_k}} - \bar{k}_i\sum_{l=1}^{L}\sum_{m=1}^{M}\Delta\Omega^{lm}\overline{I}^{lm}_{i,\Delta\eta_k}\right) \quad (28)$$

where L (=8) and M (=12) are the total number of discrete polar angle and azimuthal angle respectively.

3. Numerical details

The piloted methane/air turbulent non-premixed jet flame (Sandia flame D of Barlow and Frank [22]) is chosen as the simulation case. The jet diameter of Flame D burner is of 7.2 mm while the outer diameter is of 18.4 mm. The fuel jet consists of 25% CH_4 and 75% air (by volume). The piloted flame burns a mixture of C_2H_2, H_2, air, CO and N_2, with the same enthalpy and equilibrium composition as methane/air at 0.77 equivalence ratio. The temperatures of fuel jet, piloted flame and air co-flow are 294 K, 1880 K and 291 K respectively while the mean velocities of which are 49.6(±2 m/s), 11.4(±0.5 m/s) and 0.9 m/s, respectively. The fuel jet Reynolds number is 22,400.

The space marching algorithm is employed to solve the problem, the axial coordinate x being viewed as time-like coordinate. The governing equations for mean velocity

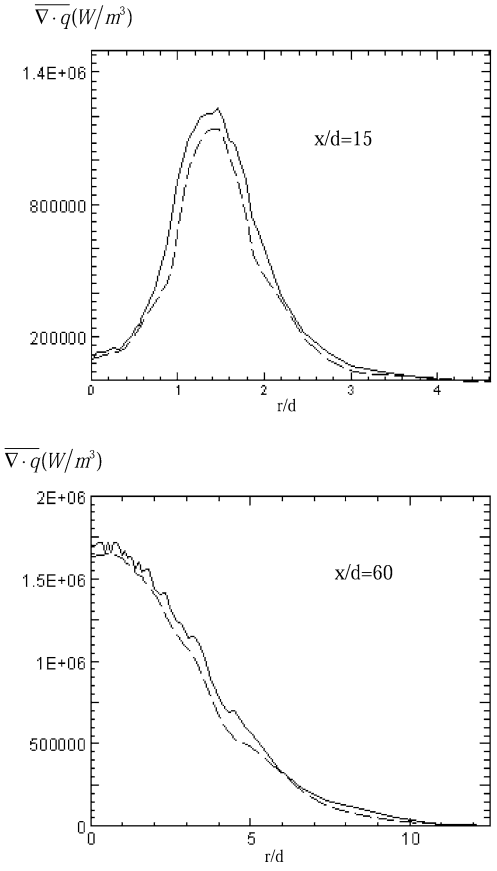

Fig. 1. Radial profiles of radiative heat loss, solid lines correspond to results with radiation, long dashed lines correspond to results without radiation.

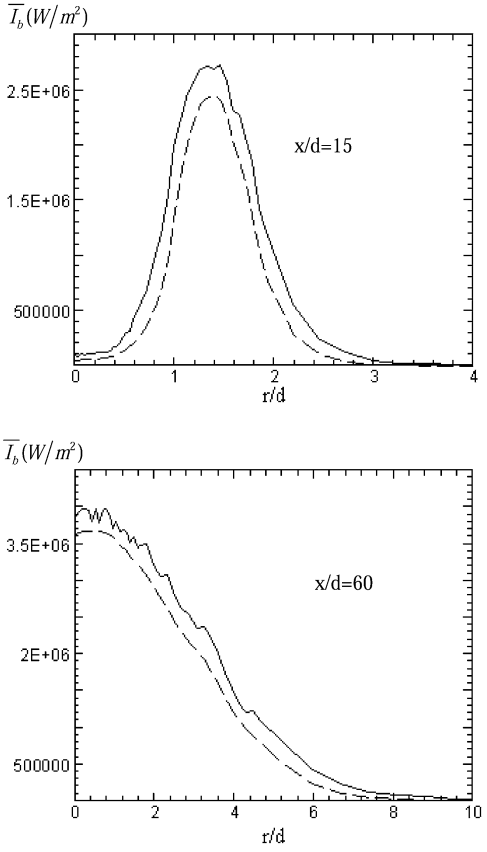

Fig. 2. Radial profiles of Plank function, solid lines correspond to results with radiation, long dashed lines correspond to results without radiation.

and turbulence are discretized by finite volume (FV) method, namely upwind difference for convection terms, central difference for diffusion terms and implicit scheme for axial convection. The obtained algebraic equations are solved by iteration. The radial velocity is deduced from the continuum equation. Along the radial direction the computational domain is divided into 50 cells. The step size along axial direction is fixed to be $\Delta x/D = 0.05$ within the whole computational domain except for the beginning part, where $\Delta x/D = 0.005$. It takes about 2000 steps to march from the nozzle to where $x = 80D$. The PDF transportation equation for mixture fraction is solved by the node-based Monte Carlo particle method [20] with 400 particles for each node. In the solution of flamelet equations, the mixture fraction space is divided into 60 cells.

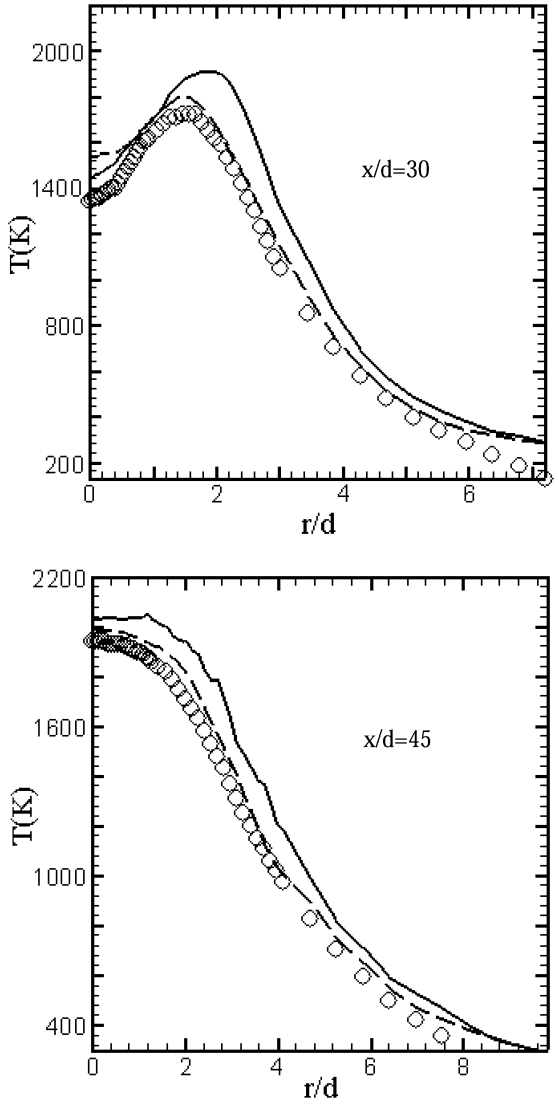

Fig. 3. Measured and calculated radial profiles. Circles denote experimental data, solid lines correspond to computation results without radiation, long dashed lines correspond to computation results with radiation.

4. Results and discussion

4.1. TRI effects in thermal radiation

Fig. 1 compares radial profiles of radiative heat loss computed by taking full TRI into account with those calculated basing on mean temperatures and mean molar fractions while Fig. 2 compares Plank function for these two cases.

When full TRI is taken into accounted, the absorption coefficient, the Plank function and the correlation of absorption coefficient and Plank function are calculated according to the following equations respectively:

$$\bar{k}_i = \int_0^1 k_i(T(f), X_s(f)) p(f)\,\mathrm{d}f \tag{29}$$

$$\overline{I_{\mathrm{b},\Delta\eta_k}} = \frac{1}{\Delta\eta_k}\int_{\Delta\eta_k} I_{\mathrm{b},\Delta\eta_k}(T(f),\eta) p(f)\,\mathrm{d}f \tag{30}$$

$$\overline{k_i I_{\mathrm{b},\Delta\eta_k}} = \int_0^1 \left(k_i(T(f),X_s(f)) \times \left(\frac{1}{\Delta\eta_k}\int_{\Delta\eta_k} I_{\mathrm{b},\Delta\eta_k}(T(f),\eta) \right) p(f)\,\mathrm{d}f \right) \tag{31}$$

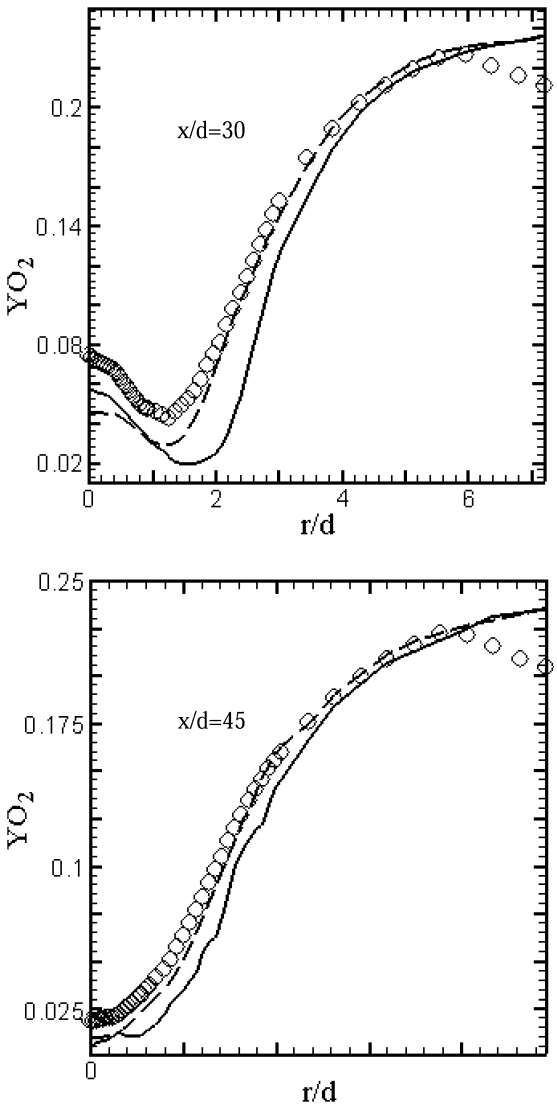

Fig. 3 (*continued*)

Correspondingly, when TRI is overlooked and the calculation is based on mean values, those terms mentioned above are calculated as follows:

$$\bar{k}_i \approx k_i(\overline{T}, \overline{X}_s) \tag{32}$$

$$\overline{I_{\mathrm{b},\Delta\eta_k}} \approx I_{\mathrm{b},\Delta\eta_k}(\overline{T}) \tag{33}$$

$$\overline{k_i I_{\mathrm{b},\Delta\eta_k}} \approx k_i(\overline{T}, \overline{X}_s) I_{\mathrm{b},\Delta\eta_k}(\overline{T}) \tag{34}$$

From Figs. 1 and 2, it can be seen that TRI tends to enhance Plank function and radiative heat loss as well. According to our calculation, radiative heat loss is enhanced by about 6.2% because of TRI while Plank function is enhanced by about 10%. Since Sandia flame D is a small flame, TRI may not account for as big a part as in practical flames. However, for detailed simulation, it is recommended that TRI should be taken into consideration.

4.2. The influence of thermal radiation

In this section, numerical results of flame D, which are calculated both with and without radiation influence, are presented and compared with the measurements. Because of the space limitation, only radial profiles of mean temperature and mean mass fraction of O_2, H_2O, CO, CO_2 and NO at two different locations along the axis are given. Fig. 3 shows that numerical simulation tends to overpredict the temperature field and the emission of reaction production (CO_2, CO, NO) and correspondingly the reaction reactant (O_2) are underpredicted. That means in our calculation, chemical reactions tend to be faster than what have been shown by measurements. The discrepancy between the computed results and experimental data may stem from the small-scale mixing model EMST. Although EMST has many advantages [21], there is still possibility that EMST may not describe the small-scale mixing

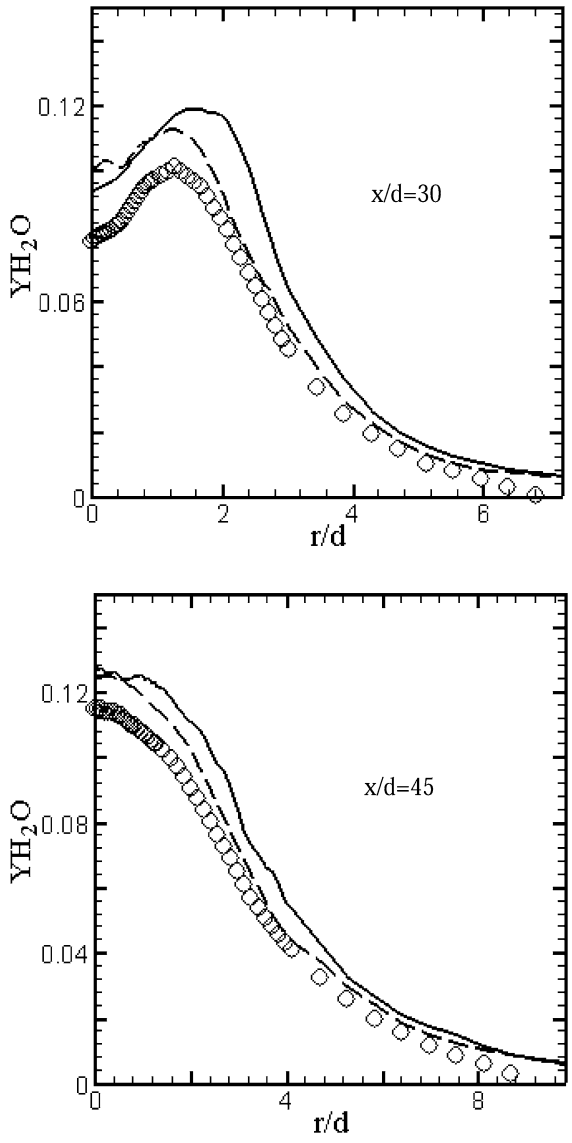

Fig. 3 (*continued*)

Fig. 3 (*continued*)

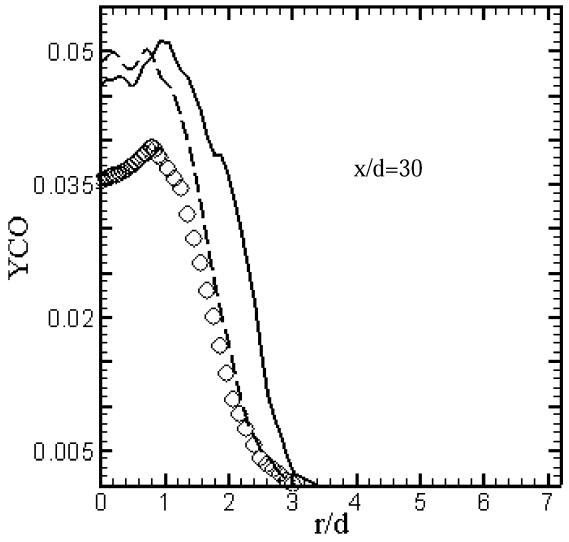

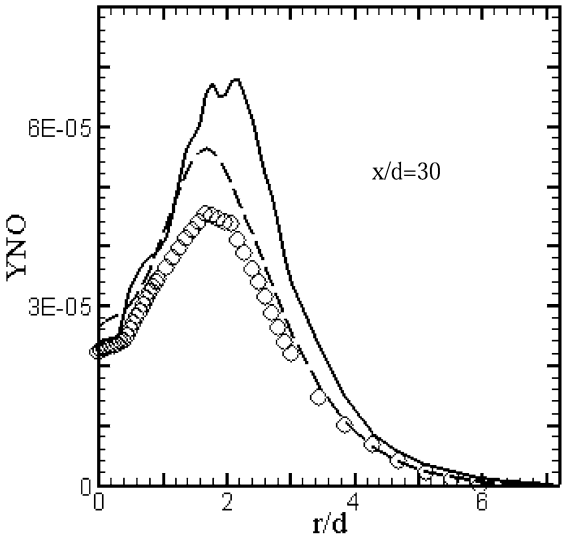

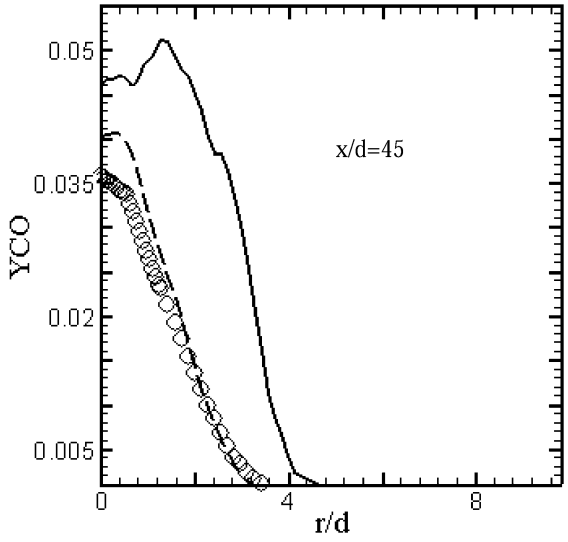

Fig. 3 (*continued*)

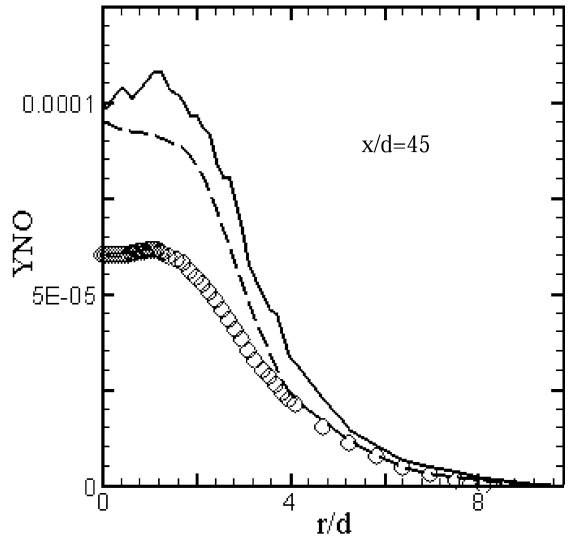

Fig. 3 (*continued*)

process as good as numerical simulation required. Another source of discrepancy is Lagrangian flamelet model (LFM), which we choose as a substitute for pure PDF method because of computation cost consideration. Basing on our own numerical experience, although LFM is superior to steady flamelet model (SFM), pure PDF method is still a little better than LFM when accuracy alone is the consideration. And although a detailed chemical mechanism instead of a simplified one is used here, still, it may not efficient enough to present the true nature of chemical reactions. At least for the prediction of NO, there are reports [22,23] that the mechanism GRI 3.0 tends to overpredict the emission of it.

However, compared with calculation reported by other researchers [24,25], our calculation gives agreeable results and with thermal radiation being taken into account, the agreement of numerical results and experiment data has been improved greatly.

An interesting phenomenon has been captured in our calculation, which, to our best knowledge, has not been reported by other researchers. The total flame radiation of flame D was measured by using a heat flux radiometer and was observed as 0.887 kW. In our calculation, the total radiation of flame D is about 1.005 kW, 13.3% higher than the measured value. Li [25] have reported their calculated heat loss of 0.798 kW while Coelho has reported his of 0.911 kW. The reasonable agreements of our result with the measured value and other reports indicate the reliability of our radiation models. It can be seen that compared with chemical reaction source term, only small amounts of energy being lost by thermal radiation and it is fair to make a assumption that in small flames as Sandia Flame D, the influence of thermal radiation is small (NO prediction being ruled out). However, basing on our calculation, although the magnitude of thermal radiation is small, the influence of radiation on the numerical result is by all means not so small. From Fig. 3, it can be seen that, taking the influence of thermal radiation into account improves the accuracy of the numerical results greatly. After the

influence of thermal radiation being taken into accounted, the problem of "burning faster than what actually is" has been solved to a great extent. Numerical results of temperature field and oxidant (O_2) mass fraction agree with measurements perfectly and except for small regions near the axis, numerical results of reaction production (H_2O, CO_2) mass fraction are with great agreement with measurements. Even for the prediction of CO and NO, which is a tough task by now, the numerical results are agreeable.

The phenomenon mentioned above is interesting yet somehow strange and a possible explanation may be that the processes of turbulence, combustion and thermal radiation are extremely depending on each other, and any small influence from thermal radiation may be magnified by the strong non-linear turbulence fluctuations and chemical reactions. Basing on our calculation, we suggested that if computation cost is not a main consideration, in turbulence combustion calculations, the influence of thermal radiation should be taken into account and perhaps detailed radiation model other than optically thin assumption should be preferred.

5. Conclusion

Sandia flame D is numerically simulated here with multiple-time scale (MTS) k–ε turbulence model for turbulence, the combination of PDF method, LFM and the detailed chemical reaction mechanism GRI 3.0 for combustion, FV/CK for radiation heat transfer. Numerical results show that TRI do enhance radiative emission as well as radiative heat loss. Though for small flames, TRI may not account for a big part, for the purpose of detailed numerical simulation, the effects of TRI are recommended to be considered. And by comparing our numerical results with measurements, it is found that although the magnitude of thermal radiation is relatively small, its influence cannot be overlooked. By taking thermal radiation into accounted, numerical accuracy has been improved greatly. Our explanation for this phenomenon is that in turbulent combustion, the process of turbulence, combustion and heat transfer are strongly depended on each other and the small influence of thermal radiation may be magnified by the non-linear processes of turbulence and combustion.

Acknowledgements

The financial support of the national Natural Science Foundation of China (50206021) is grateful acknowledged. And we are also grateful to Dr. R.S. Barlow for providing us the experimental data for scalar fields and to EM2C Lab for providing us parameters of CK model.

References

[1] R. Borghi, Turbulent combustion modeling, Prog. Energy Combust. Sci. 14 (1988) 245–292.
[2] P.A. Libby, F.A. Wiliams, Turbulent Reacting Flows, Academic Press, San Diego, 1994.
[3] S.B. Pope, PDF methods for turbulent reactive flows, Prog. Energy Combust. Sci. 11 (1985) 119–192.
[4] Available from: <http://www.me.berkeley.edu/gri_mech/>.
[5] H. Pitsch, M. Chen, N. Peters, Unsteady flamelet modeling of turbulent hydrogen–air diffusion flames, in: Twenty-seventh Symposium (International) on Combustion, The Combustion Institute, 1988, pp. 1057–1064.
[6] M.F. Modest, Radiative Heat Transfer, McGraw-Hill, New York, 1993.
[7] A. Soufiani, J. Taine, High temperature gas radiative property parameters of statistical narrow-band model for H_2O, CO_2 and CO, and correlated-K model for H_2O and CO_2, Int. J. Heat Mass Transfer 40 (1997) 987–991.
[8] S. Mazumder, M.F. Modest, A PDF approach to modeling turbulence–radiation interactions in nonluminous flames, Int. J. Heat Mass Transfer 42 (1998) 971–991.
[9] G. Li, M.F. Modest, Application of composition PDF methods in the investigation of turbulence–radiation interactions, J. Quant. Spectrosc. Radiative Transfer 73 (2002) 461–472.
[10] Fifth International Workshop on Measurement and Computation of Turbulent Nonpremixed Flames, Delft, 2000.
[11] P.J. Coelho, Detailed numerical simulation of radiative transfer in a nonluminous turbulent jet diffusion flame, Combust. Flame 136 (2004) 481–492.
[12] G. Li, M.F. Modest, Modeling and Simulation of Turbulent Heat Transfer, WIT Press, Southampton, England, 2004.
[13] P.J. Coelho, O.J. Teerling, D. Roekaerts, Spectral radiative effects and turbulence-radiation-interaction in Sandia flame D, TNF6_ proceedings, 2002.
[14] S.W. Kim, C.P. Chen, A multiple-time-scale turbulence model based on variable partitioning of the turbulent kinetic energy spectrum, Numer. Heat Transfer, Part B 16 (1989) 193–211.
[15] H.F. Wang, Y.L. Chen, PDF modeling of turbulent non-premixed combustion with detailed chemistry, Chem. Eng. Sci. 59 (2004) 3477–3490.
[16] N. Peters, Laminar diffusion flamelet models in non-premixed turbulent combustion, Prog. Energy Combust. Sci. 10 (1984) 319–339.
[17] Z.Y. Ren, S. Subramaniam, S.B. Pope, Implementation of the EMST mixing model, Available from: <http://mae.cornell.edu/~laniu/emst>.
[18] F.S. Liu, G.J. Smallwood, Application of the statistical narrow-band correlated-k method to non-grey gas radiation in CO_2–H_2O mixtures: approximate treatments of overlapping bands, J. Quant. Spectrosc. Radiative Transfer 68 (2001) 401–417.
[19] V.P. Kabashnikov, G.I. Myasnikova, Thermal radiation in turbulent flows—temperature and concentration fluctuations, Heat Transfer Sov. Res. 17 (1985) 116–125.
[20] S.B. Pope, Monte Carlo method for the PDF equations of turbulent reactive flow, Combust. Sci. Tech. 25 (1981) 159–174.
[21] Z.Y. Ren, S.B. Pope, An investigation of the performance of turbulent mixing models, Combust. Flame 136 (2004) 208–216.
[22] R.S. Barlow, J.H. Frank, Effects of turbulence on species mass fractions in methane/air jet flames, in: Twenty-seventh Symposium (International) on Combustion, 1998, pp. 1087–1095.
[23] V. Raman, R.O. Fox, A.D. Harvey, Hybrid finite-volume/transported PDF simulation of a partially premixed methane–air flame, Combust. Flame 136 (2004) 327–350.
[24] International Workshop on Measurement and Computation of Turbulent Non-premixed Flames, Available from: <http://www.ca.sandia.gov/tdf/workshop.html>.
[25] G. Li, Investigation of turbulence-radiation interactions by a hybrid FV/PDF Monte Carlo method, Ph.D. thesis, The Pennsylvania State University, 2002.